PHYSICAL REVIEW B **92**, 094513 (2015)

Enhanced superconducting transition temperature in hyper-interlayer-expanded FeSe despite the suppressed electronic nematic order and spin fluctuations

Matevž Majcen Hrovat,[1] Peter Jeglič,[1] Martin Klanjšek,[1] Takehiro Hatakeda,[2] Takashi Noji,[2] Yoichi Tanabe,[3]
Takahiro Urata,[3] Khuong K. Huynh,[3] Yoji Koike,[2] Katsumi Tanigaki,[3,4] and Denis Arčon[1,5,*]
[1]*Jožef Stefan Institute, Condensed Matter Physics Department, Jamova cesta 39, SI-1000 Ljubljana, Slovenia*
[2]*Department of Applied Physics, Tohoku University, 6-6-05 Aoba, Aramaki, Aoba-ku, Sendai 980-8579, Japan*
[3]*Department of Physics, Graduate School of Science, Tohoku University, 6-6-05 Aoba, Aramaki, Aoba-ku, Sendai 980-8579, Japan*
[4]*World Premier Institute - Advanced Institute for Materials Research, Tohoku University, 2-1-1 Katahira, Aoba-ku, Sendai 980-8578, Japan*
[5]*Faculty of Mathematics and Physics, University of Ljubljana, Jadranska cesta 19, SI-1000 Ljubljana, Slovenia*

(Received 3 August 2015; published 23 September 2015)

The superconducting critical temperature, T_c, of FeSe can be dramatically enhanced by intercalation of a molecular spacer layer. Here we report on a ^{77}Se, ^{7}Li, and ^{1}H nuclear magnetic resonance (NMR) study of the powdered hyper-interlayer-expanded $Li_x(C_2H_8N_2)_yFe_{2-z}Se_2$ with a nearly optimal $T_c = 45$ K. The absence of any shift in the ^{7}Li and ^{1}H NMR spectra indicates a complete decoupling of interlayer units from the conduction electrons in FeSe layers, whereas nearly temperature-independent ^{7}Li and ^{1}H spin-lattice relaxation rates are consistent with the non-negligible concentration of Fe impurities present in the insulating interlayer space. On the other hand, the strong temperature dependence of ^{77}Se NMR shift and spin-lattice relaxation rate, $1/^{77}T_1$, is attributed to the holelike bands close to the Fermi energy. $1/^{77}T_1$ shows no additional anisotropy that would account for the onset of electronic nematic order down to T_c. Similarly, no enhancement in $1/^{77}T_1$ due to the spin fluctuations could be found in the normal state. Yet, a characteristic power-law dependence $1/^{77}T_1 \propto T^{4.5}$ still complies with the Cooper pairing mediated by spin fluctuations.

DOI: 10.1103/PhysRevB.92.094513 PACS number(s): 74.70.Xa, 74.25.nj, 74.20.Mn

I. INTRODUCTION

The discovery of superconductivity in a layered iron oxypnictide [1] has triggered an intensive research activity to optimize the unconventional superconducting properties of iron-based superconductors. Changing the composition of iron-based superconductors led to two distinct families, iron pnictides and iron chalcogenides, that share the same structural motif of electronically active layers composed of FeAs and FeQ (Q = Se, Te) tetrahedra, respectively. A binary $Fe_{1+\delta}Se$ adopts a particularly simple PbO-type structure [2], where the structural tetragonal-to-orthorhombic transition at $T_s = 91$ K [3] is, unlike as in 1111 or 122 FeAs compounds [4], not accompanied by the spin-density-wave (SDW) magnetic ordering. However, below T_s the rotational (C_4) symmetry is broken as the electronic nematic order [4–10] is established, thus raising important questions regarding the absence of SDW: What triggers the electronic nematic order and what are its implications for the superconductivity in the iron-chalcogenide family?

The two main candidates that may drive the electronic nematic order are electron spin and orbital degrees of freedom. Pronounced splitting of ^{77}Se nuclear magnetic resonance (NMR) spectra in high-quality FeSe single crystals below T_s has a characteristic order parameter temperature dependence and has been associated with symmetry lowering due to the orbital ordering [3,10]. The simultaneous absence of enhancement of the ^{77}Se spin-lattice relaxation rate due to the spin fluctuations close to T_s implies that the orbital degrees of freedom drive the nematic order [10]. High-resolution angle-resolved photoemission spectroscopy (ARPES) found dramatic changes in the electronic structure below T_s that corroborate the electronically driven transition, which is stabilized by orbital ordering [9]. On the other hand, a recent neutron scattering study revealed substantial stripe spin fluctuations that are coupled with orthorhombicity and enhanced close to T_s, thus favoring spin fluctuations as the driving mechanism for the nematicity [11]. This latter possibility also seems to be more consistent with the theoretical studies that predict the nematic quantum paramagnetic state [12] with spin fluctuations at $\mathbf{q} = (\pi, Q)$ (where $Q = 0, \pi/4, \pi/3, \pi/2, ...$) [13]. The high energy of spin fluctuations renders them unobservable by NMR, thus explaining the absence of a significant enhancement of the spin-lattice relaxation rate close to T_s.

$Fe_{1+\delta}Se$ is a superconductor with a critical temperature $T_c \approx 8$ K at ambient pressure [2,3,10,14,15]. With the application of hydrostatic pressure, T_c dramatically increases, reaching the maximum of 37 K at ~7 GPa [16]. Strikingly, single FeSe layers grown on $SrTiO_3$ show superconductivity at even higher temperatures, in some cases at critical temperatures that exceed 100 K [17,18]. Significant enhancement of T_c is also observed in FeSe structures intercalated with alkali metal coordinated to molecular spacers (e.g., ammonia, pyridine, ethylenediamine, or hexamethylenediamine) [19–26], where T_c first nearly linearly increases with increasing interlayer spacing d between 5 and 9 Å, and then roughly saturates at $T_c \approx 45$ K for $d > 9$ Å [23]. The degree of Fe vacancies in the FeSe layer and the non-negligible amount of Fe intercalated between FeSe layers were found to influence the superconducting properties of lithium iron selenide hydroxides $Li_{1-x}Fe_x(OH)Fe_{1-y}Se$ [26]. Detailed *ab initio* calculations indeed support this picture by finding that the Li atoms donate electrons to the FeSe layer, thus tuning the critical temperature [27]. Interestingly, Fe ions present in the layers separating FeSe layers may ferromagnetically order at low temperature [28,29],

---

[*] denis.arcon@ijs.si

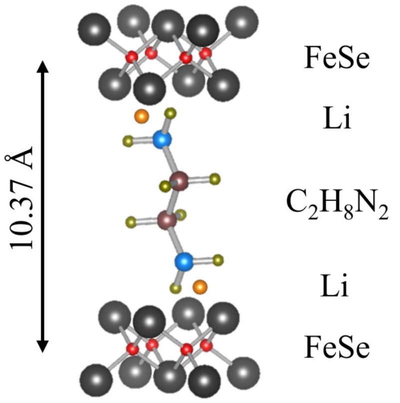

FIG. 1. (Color online) Schematic crystal structure of the intercalated FeSe-based $Li_x(C_2H_8N_2)_yFe_{2-z}Se_2$ compound with the hyperexpanded distance between neighboring Fe layers of $d = 10.37$ Å and enhanced superconducting critical temperature $T_c = 45$ K. Here, red spheres represent Fe, gray spheres Se, orange spheres Li, blue spheres N, brown spheres C, and green spheres H. The position of impurity Fe atoms in the interlayer space is unknown.

thus reminiscing the magnetic ordering of interlayer rare-earth moments in the 1111 family, e.g., in NdOFeAs [30].

How various factors such as (i) disorder (ion vacancies, intercalated Fe, or simply the structural disorder related to the co-intercalated molecular coordination), (ii) dimensionality, (iii) spin fluctuations, and (iv) possible nematicity vary across the intercalated-FeSe phase diagram is still unclear. Here we report a systematic ^{77}Se, ^{7}Li, and ^{1}H NMR study of hyper-interlayer-expanded (lattice constant $c = 20.74$ Å yields $d = 10.37$ Å) Li co-intercalated with ethylenediamine composition $Li_x(C_2H_8N_2)_yFe_{2-z}Se_2$ (i-FeSe), Fig. 1, with a superconducting critical temperature $T_c = 45$ K [20]. Probing the intra- and interlayer properties, we find that the studied i-FeSe with nearly optimal T_c should indeed be treated as a two-dimensional electronic system, which is not significantly perturbed by the considerable disorder present in the interlayer space. The absence of enhanced spin fluctuations and (within the resolution of powder NMR data) of nematic order provide important constraints for the superconducting state in the studied i-FeSe.

II. EXPERIMENTAL METHODS

Samples were prepared according to standard procedures described in detail in Ref. [20]. Powder x-ray diffraction confirmed that the samples were composed of Li- and ethylenediamine-co-intercalated $Li_x(C_2H_8N_2)_yFe_{2-z}Se_2$ with some minor unreacted FeSe impurity. The low-field magnetization measurements disclosed two superconducting transitions, the first at $T_c = 45$ K belonging to i-FeSe and the second due to nonintercalated FeSe impurity at $T_c = 8$ K [20]. We note that the presence of the nonintercalated FeSe phase seems to be unavoidable in these materials [20,23].

^{77}Se ($I = 1/2$) NMR experiments were conducted in a magnetic field of 9.4 T. The reference Larmor frequency of $\nu_L(^{77}\text{Se}) = 76.282$ MHz was determined from Me_2Se standard. A two-pulse Hahn-echo sequence $\pi/2$-τ-π-echo with a $\pi/2$ pulse length of 7 μs and an interpulse delay $\tau = 50\,\mu$s was employed. ^{7}Li ($I = 3/2$) and ^{1}H ($I = 1/2$) NMR measurements were performed in a magnetic field of 2.35 T at Larmor frequencies $\nu_L(^{7}\text{Li}) = 38.85$ MHz (LiCl has been taken as a reference standard) and $\nu_L(^{1}\text{H}) = 99.95$ MHz. For the ^{7}Li quadrupole nuclei a two-pulse solid-echo sequence $\pi/2$-τ-$\pi/2$-echo with a $\pi/2$ pulse length of 4.4 μs and an interpulse delay $\tau = 30\,\mu$s has been used. ^{1}H NMR frequency-swept spectra were recorded in 50-kHz steps of irradiation frequency with the two-pulse Hahn-echo sequence ($\pi/2$ pulse length was 8 μs and $\tau = 20$ μs). The ^{77}Se, ^{7}Li, and ^{1}H spin-lattice relaxation rates, $1/^{77}T_1$, $1/^{7}T_1$, and $1/^{1}T_1$, were measured with an inversion-recovery technique at the corresponding NMR line shape peak positions. The ^{77}Se magnetization recovery curves for the i-FeSe sample were fitted to a sum of two components in order to explicitly take into account also the presence of nonintercalated FeSe.

III. RESULTS AND DISCUSSION

The room-temperature ^{1}H and ^{7}Li NMR spectra are featureless, symmetric, and centered close to their Larmor frequencies (Fig. 2). The absence of a measurable shift in the ^{7}Li NMR spectrum implies an almost fully ionized Li^+ species and a complete charge transfer to the FeSe layer. The linewidth of the ^{1}H NMR spectrum amounts to 2083(16) ppm at 300 K, which is an expected line broadening caused by the proton-proton dipolar interactions of co-intercalated ethylenediamine molecules. We note that the ^{7}Li NMR spectrum at 300 K exhibits a nearly identical linewidth of 2417(19) ppm, implying a similar size of the local magnetic fields at the Li site. Since Li atoms are, likewise to ethylenediamine molecules, intercalated between FeSe layers, we conclude that the proton dipolar fields also broaden ^{7}Li NMR spectra. On cooling, both ^{1}H and ^{7}Li NMR spectra show only a very moderate broadening and do not shift away from their respective Larmor frequencies. For comparison, small but nonzero ^{23}Na and ^{7}Li NMR shifts due to the weak transferred hyperfine coupling to the FeAs layer were found in NaFeAs and LiFeAs [31,32]. Moreover, the ^{1}H and ^{7}Li NMR spectra in i-FeSe are almost

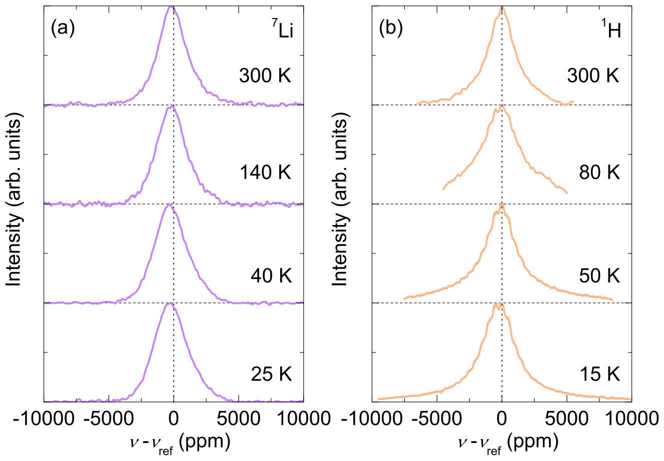

FIG. 2. (Color online) Temperature evolution of (a) ^{7}Li and (b) ^{1}H NMR spectra of i-FeSe powder. Please note the absence of shift and the similar line broadening for both nuclei. Dotted vertical lines indicate the corresponding Larmor frequencies.

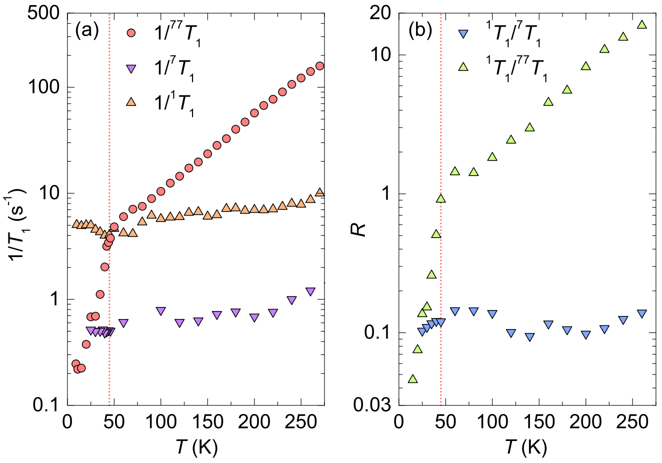

FIG. 3. (Color online) (a) Temperature dependencies of ^{1}H (orange triangles), ^{7}Li (violet upside-down triangles), and ^{77}Se (red circles) spin-lattice relaxation rates, $1/^nT_1$ ($n = 1,7,77$). (b) Temperature dependence of the ratio, R, of ^{1}H to ^{7}Li, $^1T_1/^7T_1$ (blue upside-down triangles), and of ^{1}H to ^{77}Se, $^1T_1/^{77}T_1$ (green triangles), spin-lattice relaxation times. Dotted vertical lines indicate the superconducting critical temperature $T_c = 45$ K of the i-FeSe sample.

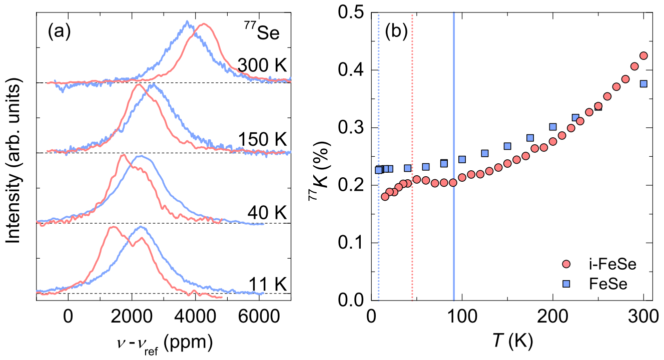

FIG. 4. (Color online) (a) Temperature evolution of the ^{77}Se NMR spectra measured in i-FeSe (red line) and in FeSe (blue line) powders. Note the presence of a second weak peak attributed to the presence of nonintercalated FeSe impurity regions in the spectra of i-FeSe. (b) Temperature dependencies of the ^{77}Se NMR shifts for i-FeSe (red circles) and FeSe (blue squares). Dotted vertical lines indicate the superconducting critical temperature $T_c = 45$ K for i-FeSe (red) and $T_c = 8$ K for FeSe (blue). The solid vertical blue line marks an FeSe structural phase transition at $T_s = 91$ K.

insensitive to the superconducting transition at $T_c = 45$ K as the corresponding small diamagnetic shift $\Delta B/B$ cannot be resolved due to the large linewidth of the spectra. These observations unambiguously prove that the Li atoms and ethylenediamine molecules feel no hyperfine field and are thus completely decoupled from the conducting electrons in FeSe layers. Their role is thus to provide charges to the FeSe layers and to separate these layers, thus establishing the i-FeSe compound as a perfect two-dimensional conductor.

^{1}H and ^{7}Li spin-lattice relaxation rates, $1/^nT_1$ (here $n = 1,7$ stands for ^{1}H and ^{7}Li, respectively) marginally decrease with deceasing temperature between room temperature and 10 K [Fig. 3(a)]. The ratio of ^{1}H to ^{7}Li spin-lattice relaxation times, $^1T_1/^7T_1$, is almost temperature independent [Fig. 3(b)], thus proving that both nuclei experience the same spectrum of fluctuating local magnetic fields and corroborating the conclusions derived from the ^{1}H and ^{7}Li NMR spectra (Fig. 2). Evidently, there is no contribution from the relaxation governed by the hyperfine coupling to the conducting FeSe electrons. This explains why $1/^nT_1$ are not sensitive to the onset of superconductivity, which would otherwise lead to a suppression of spin-lattice relaxation rates below T_c.

Establishing the absence of conducting electron hyperfine fields in the interlayer space, one can expect that the spin-lattice relaxation in this layer will be governed by other mechanisms usually encountered in insulators. In the case when spin-lattice relaxation is determined by the ethylenediamine molecular motions, the Bloembergen-Purcell-Pound (BPP)-type relaxation mechanism applies and $1/^1T_1$ should display strong thermally activated (Arrhenius-type) temperature dependence with a maximum at the temperature where the correlation time τ for the molecular motion matches the inverse Larmor frequency, i.e., when $\omega_L\tau = 1$ [33,34]. However, this is clearly not supported by the very weak temperature dependence of $1/^1T_1$ [Fig. 3(a)]. Therefore, we conclude that the ^{1}H (and likewise also ^{7}Li) spin-lattice relaxation process is cut short by another weakly temperature-dependent relaxation mechanism. A plausible possibility that provides such a nearly temperature-independent spin-lattice relaxation is a nuclear-spin diffusion toward the diluted localized magnetic moments [35]. In two-dimensional diluted paramagnets $1/^1T_1 \propto N_p D^{3/4}$, where N_p is a concentration of paramagnetic impurities and D is the nuclear spin diffusion constant [36]. The latter is given by the nuclear second moment and may thus account for the residual weak temperature dependence of $1/^1T_1$. In i-FeSe, such diluted paramagnetic impurities could be associated with the non-negligible concentration of Fe impurities present in the insulating interlayer space. However, judging from the absence of additional broadening of ^{1}H and ^{7}Li NMR spectra and the absence of $1/^1T_1$ enhancement, these Fe impurities show no tendency towards magnetic ordering down to 10 K.

Since Li and ethylenediamine species are electronically completely isolated from FeSe layers, we now turn to the ^{77}Se NMR to directly probe the electronic properties of the FeSe layer. Comparison of the ^{77}Se NMR spectra of powdered FeSe and i-FeSe samples is shown in Fig. 4(a). The linewidth of the i-FeSe spectrum is 90 kHz (which corresponds to ~1200 ppm) at 300 K and is comparable to that of the FeSe powder. The broadening due to the ^{1}H-^{77}Se dipolar interactions is estimated to be negligible compared to the hyperfine broadening between the ^{77}Se nuclear moments and the conducting electrons in the FeSe layers. In addition to the main ^{77}Se NMR line of i-FeSe, a second minor peak becomes more pronounced below ~150 K. A direct comparison with the spectra of FeSe reveals that this weaker resonance in fact belongs to ≈20% of nonintercalated FeSe regions present in our sample.

The shift of the ^{77}Se NMR spectra, ^{77}K, in i-FeSe corresponds to 4250 ppm at room temperature and is significantly larger compared to FeSe where it amounts to 3760 ppm. On cooling, $^{77}K(T)$ shows a very strong temperature dependence [Fig. 4(b)], roughly following the empirical $^{77}K(T) = K_0 + kT^2$ dependence with the fitting constants $K_0 = 1834$ ppm and $k = 0.025$ ppm/K^2. On the other hand, FeSe shows weaker temperature dependence of ^{77}K and, if analyzed with the same empirical model, a significantly smaller $k = 0.017$ ppm/K^2 (and larger $K_0 = 2279$ ppm) is obtained. In general, the shift is composed of the temperature-independent orbital contribution, $K_{\rm orb}$, and the Knight shift, $K_{\rm s}$, respectively. The Knight shift $K_{\rm s}$ is related to the density of states $g(\epsilon)$ in the vicinity of the Fermi energy $\epsilon_{\rm F}$, i.e.,

$$K_{\rm s}(T) \propto \int g(\epsilon)\left(-\frac{\partial f}{\partial \epsilon}\right) d\epsilon, \qquad (1)$$

where $f(\epsilon) = 1/(1 + \exp[(\epsilon - \epsilon_{\rm F})/k_{\rm B}T])$ is the Fermi-Dirac distribution function. When $\epsilon_{\rm F}$ is positioned somewhere in the middle of the conduction band, where $g(\epsilon)$ does not change significantly over the energy range of $k_{\rm B}T$, the above expression predicts temperature-independent $K_{\rm s}$, which is proportional to the density of states at the Fermi level, $g(\epsilon_{\rm F})$. However, $K_{\rm s}$ can become temperature dependent if $g(\epsilon)$ changes substantially in the energy interval $|\epsilon - \epsilon_{\rm F}| \sim k_{\rm B}T$. In FeSe, this condition seems to be fulfilled for the holelike pockets α, β, and γ with band edges very close to $\epsilon_{\rm F}$ according to the recent ARPES study [9]. Although no comparable ARPES study is at the moment available for our i-FeSe sample, we can qualitatively argue that the much steeper and stronger temperature dependence of $K_{\rm s}$ in i-FeSe suggests that at least one of these bands is pushed even closer to $\epsilon_{\rm F}$ upon intercalation.

A very similar conclusion is derived also from the ^{77}Se spin-lattice relaxation rates [Fig. 3(a)]. The Korringa-type relaxation

$$1/T_1T \propto \int g^2(\epsilon)\left(-\frac{\partial f}{\partial \epsilon}\right) d\epsilon \qquad (2)$$

predicts temperature-independent $1/T_1T$ rates only for the cases when band edges are far away from $\epsilon_{\rm F}$. Therefore, a very steep increase of $1/^{77}T_1T$ [Fig. 5(a)] with increasing temperature for $T > 100$ K implies that the relaxation rate is enhanced because at least one of the the holelike pockets α, β, and γ has features very close to $\epsilon_{\rm F}$. Again, the temperature dependence of $1/^{77}T_1T$ in i-FeSe is more pronounced than in FeSe, thus corroborating the conclusions derived from the discussion of the Knight shift data.

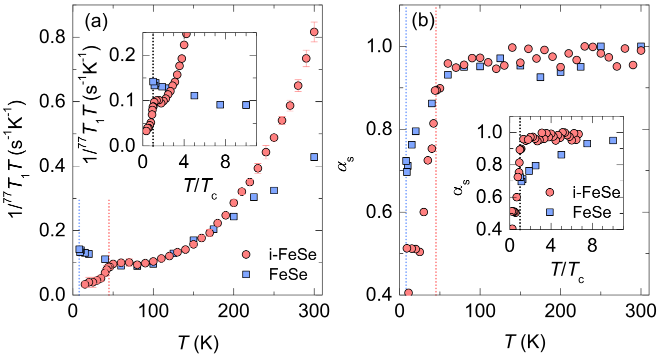

FIG. 5. (Color online) Temperature dependencies of (a) the ^{77}Se spin-lattice relaxation rates, $1/^{77}T_1$, divided by temperature and (b) of the stretching exponent $\alpha_{\rm s}$ for i-FeSe (red circles) and FeSe (blue squares). Insets to (a) and (b) show the temperature dependencies of $1/^{77}T_1T$ and $\alpha_{\rm s}$ in the reduced $T/T_{\rm c}$ scale. Dotted vertical lines indicate the superconducting critical temperature $T_{\rm c} = 45$ K for i-FeSe (red) and $T_{\rm c} = 8$ K for FeSe (blue). Dotted vertical black lines in the insets mark the onset of superconductivity where $T/T_{\rm c} = 1$.

Slight shifting of the holelike pockets α, β, and γ in i-FeSe compared to FeSe samples may also be responsible for an important difference between the temperature dependencies of $1/^{77}T_1T$ in the two samples below $T \approx 100$ K. Namely, in FeSe $1/^{77}T_1T$ starts to increase with decreasing temperature in the electronic nematic phase below the structural phase transition $T_{\rm s} = 91$ K [Fig. 5(a)], in agreement with the literature data [3,10,37]. Such an enhancement of the relaxation rate is a strong indication of the enhancement in the spectral density function of spin fluctuations at the nuclear Larmor frequency. Similarly as in many iron pnictide compounds [38–40], the increase in $1/^{77}T_1T$ is accompanied by the larger distribution of $1/^{77}T_1$ values. In iron pnictides the distribution of spin-lattice relaxation rates is due to the inhomogeneous glassy dynamics [38]. However, this is very unlikely in the case of FeSe, which is far away from the SDW instability. Therefore, we attribute the distribution in $1/^{77}T_1$ in FeSe to the larger anisotropy in $1/^{77}T_1$ in the electronic nematic phase [3,10]. In the present experiments on powdered samples this is evident from the stretched-exponential form of the ^{77}Se nuclear magnetization recovery data with the stretching exponent $\alpha_{\rm s}$ decreasing from 0.96(8) for $T_{\rm s} < T < 300$ K to 0.73(5) at $T_{\rm c} = 8$ K [Fig. 5(b)]. Returning to the i-FeSe sample, we first notice that the enhancement in $1/^{77}T_1T$ is absent down to the superconducting critical temperature $T_{\rm c} = 45$ K. Moreover, although $\alpha_{\rm s}$ is seemingly similar in both compounds, we emphasize that within experimental accuracy in i-FeSe it remains constant between room temperature and $T_{\rm c} = 45$ K. We note that $T_{\rm c}$ defines the energy scale of the superconducting correlations against which the strength of competing spin or nematic fluctuations has to be compared. Therefore, we next plot $1/^{77}T_1T$ and $\alpha_{\rm s}$ parameters in the reduced $T/T_{\rm c}$ scale [insets to Figs. 5(a) and 5(b)]. Now, the differences in the temperature dependencies of both parameters between the two compounds become very pronounced. Whereas in FeSe the enhancement in $1/^{77}T_1T$ and the suppression of $\alpha_{\rm s}$ can be tracked up to $T/T_{\rm c} \approx 10$, in i-FeSe $1/^{77}T_1T$ and $\alpha_{\rm s}$ remain nearly temperature independent at 0.097(8) s^{-1} K^{-1} and 0.95(5) between $T/T_{\rm c} = 1$ and $T/T_{\rm c} \approx 2$, respectively. This suggests the suppression of spin fluctuations probed at the NMR frequency and the absence of anisotropy in the electronic response, the latter speaking for the suppression of electronic nematic order, in the normal state of i-FeSe.

A comparative NMR study of i-FeSe and FeSe in the normal state discloses some important electronic differences between the two compounds: (i) at least some of the holelike pockets in i-FeSe shift closer to $\epsilon_{\rm F}$, (ii) there is a suppression of spin fluctuations probed at the nuclear Larmor frequency, and (iii) (within the resolution of present powder experiments) there is also a suppression of nematicity in i-FeSe. These differences are expected to be reflected also in the superconducting state. For instance, if spin fluctuations mediate the Cooper pairing, the system is predicted to develop an unconventional $s^{\pm}$ superconductivity [41]. On the other hand, when orbital fluctuations are in play, then the s^{++} state is predicted [42]. Moreover, since it was suggested that the nematicity competes with the superconductivity in FeSe [3], our finding of suppressed electronic nematicity may at least

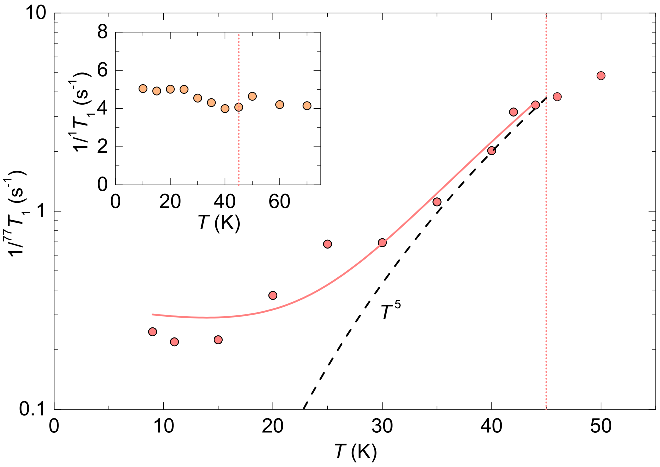

FIG. 6. (Color online) Temperature dependence of ^{77}Se spin-lattice relaxation rate, $1/^{77}T_1$, below the i-FeSe superconducting critical temperature $T_c = 45$ K. The dashed line shows the expected temperature dependence for a power law $1/^{77}T_1 \propto T^5$ compatible with the $s^{\pm}$ superconductivity. Solid red line is a fit to $1/^{77}T_1 = A + B(T/T_c)^n$ with $A = 0.24$ s^{-1}, $B = 3.39$ s^{-1}, and $n = 4.5$. Inset: ^{1}H spin-lattice relaxation rate, $1/^{1}T_1$, is nearly temperature independent below T_c. Thin dotted vertical lines mark T_c.

qualitatively account for the high T_c in i-FeSe. In Fig. 6 we show the low-temperature dependence of $1/^{77}T_1$. A sharp suppression of $1/^{77}T_1$ below T_c confirms the opening of the superconducting gap and reveals the absence of a characteristic spin-lattice relaxation rate enhancement due to the coherence peak just below T_c. We stress that for the s^{++} superconducting state the coherence peak would be expected. However, as it has been observed in isotropic s-wave strongly correlated systems [43,44], the damping effects arising from the scattering of the electron with other electrons may suppress the coherence peak. Although electron correlations have been discussed in iron chalcogenides [45–47], it is still unlikely that they are strong enough to account for the experimental observation of the completely suppressed coherence peak. Therefore, we consider the orbital fluctuations s^{++} scenario in i-FeSe less probable.

Below T_c, $1/^{77}T_1$ adopts a power-law temperature dependence, $1/^{77}T_1 \propto T^n$. Such a power-law dependence can be found for most iron pnictides [48–52] and iron chalcogenides [53] with n varying from 3 to 5. Various models based on $s^{\pm}$-wave symmetry with the two Fermi surfaces dominated by an isotropic full and an anisotropic full gap can account for such dependence [52]. Indeed, fitting $1/^{77}T_1$ of i-FeSe below T_c to $1/^{77}T_1 \propto T^n$ with $n \approx 5$ provides a satisfactory fit of the data (Fig. 6). However, at the lowest temperatures below ∼15 K, when the main relaxation channel via thermally excited quasiparticles becomes very weak, $1/^{77}T_1$ suddenly tends to saturate. This is reminiscent of nearly temperature independent ^{1}H (and also ^{7}Li) relaxation rates (inset to Fig. 6), thus implying that very weak fluctuating fields originating from the interlayer impurity Fe magnetic moments provide an additional relaxation channel for the ^{77}Se nuclei. Therefore, we fit $1/^{77}T_1$ to a sum of two contributions, $1/^{77}T_1 = A + B(T/T_c)^n$, for all $T < T_c$. Here, A and B are the fitting constants related to the magnitude of the fluctuating insulating interlayer moments and to the hyperfine fields from the electrons in the FeSe layer, respectively. Finally, the extracted $n = 4.5$ is in qualitative agreement with the $s^{\pm}$ scenario.

We remark that the presence of an additional temperature-independent relaxation channel in i-FeSe introduces some uncertainty to the extracted fitting parameters in the superconducting state. Nevertheless, most of the NMR data still seem to be compatible with the Cooper pairing mediated by spin fluctuations. This may be in apparent contradiction with the observation of suppressed spin fluctuations in the normal state [Fig. 5(a)]. However, if the theoretical suggestion that spin fluctuations are very high in energy is correct [12], then their influence on the nuclear spin relaxation would be negligible and could still account for the very high T_c in i-FeSe. Our finding that the holelike pockets shift closer to ϵ_F in i-FeSe may then hold important clues about the tuning of spin fluctuations and optimizing T_c in this family of materials.

In conclusion, $Li_x(C_2H_8N_2)_yFe_{2-z}Se_2$ with a superconducting critical temperature $T_c = 45$ K has been studied with ^{77}Se, ^{7}Li, and ^{1}H NMR. Electronically active FeSe layers are found to be completely decoupled from each other by insulating layers comprising ethylenediamine, Li, and, importantly, also intercalated (impurity) Fe atoms. In comparison to the parent FeSe, i-FeSe shows completely suppressed electronic nematicity and the absence of spin fluctuations probed at the NMR Larmor frequency. However, the Cooper pairing mediated by high-energy spin fluctuations still provides the best explanation for the absence of the coherence peak and the power-law dependence of the spin-lattice relaxation rates below T_c. The family of intercalated FeSe compounds thus emerges as an intriguing case where the intertwining of lattice, charge, and spin degrees of freedom establishes a highly intricate superconducting state with surprisingly high T_c.

ACKNOWLEDGMENTS

D.A. acknowledges the financial support from the European Union FP7-NMP-2011-EU-Japan project LEMSUPER under Contract No. NMP3-SL-2011-283214 and from the Slovenian Research Agency project under Contract No. BI-JP/12-14-003.

---

[1] Y. Kamihara, T. Watanabe, M. Hirano, and H. Hosono, J. Am. Chem. Soc. **130**, 3296 (2008).

[2] F.-C. Hsu, J.-Y. Luo, K.-W. Yeh, T.-K. Chen, T.-W. Huang, P. M. Wu, Y.-C. Lee, Y.-L. Huang, Y.-Y. Chu, D.-C. Yan *et al.*, Proc. Natl. Acad. Sci. USA **105**, 14262 (2008).

[3] S.-H. Baek, D. V. Efremov, J. M. Ok, J. S. Kim, J. van den Brink, and B. Büchner, Nat. Mater. **14**, 210 (2015).

[4] P. Dai, J. Hu, and E. Dagotto, Nat. Phys. **8**, 709 (2012).

[5] J. Hu and C. Xu, Phys. C (Amsterdam, Neth.) **481**, 215 (2012).

[6] X. Lu, J. T. Park, R. Zhang, H. Luo, A. H. Nevidomskyy, Q. Si, and P. Dai, Science **345**, 657 (2014).

[7] R. M. Fernandes, A. V. Chubukov, and J. Schmalian, Nat. Phys. **10**, 97 (2014).

[8] J.-H. Chu, H.-H. Kuo, J. G. Analytis, and I. R. Fisher, Science **337**, 710 (2012).

[9] M. D. Watson, T. K. Kim, A. A. Haghighirad, N. R. Davies, A. McCollam, A. Narayanan, S. F. Blake, Y. L. Chen, S. Ghannadzadeh, A. J. Schofield *et al.*, Phys. Rev. B **91**, 155106 (2015).

[10] A. Böhmer, T. Arai, F. Hardy, T. Hattori, T. Iye, T. Wolf, H. Löhneysen, K. Ishida, and C. Meingast, Phys. Rev. Lett. **114**, 027001 (2015).

[11] Q. Wang, Y. Shen, B. Pan, Y. Hao, M. Ma, F. Zhou, P. Steffens, K. Schmalzl, T. R. Forrest, M. Abdel-Hafiez *et al.*, arXiv:1502.07544.

[12] F. Wang, S. A. Kivelson, and D.-H. Lee, Nat. Phys. (2015).

[13] J. K. Glasbrenner, I. I. Mazin, H. O. Jeschke, P. J. Hirschfeld, R. M. Fernandes, and R. Valentí, Nat. Phys. (2015).

[14] S. Margadonna, Y. Takabayashi, M. T. McDonald, K. Kasperkiewicz, Y. Mizuguchi, Y. Takano, A. N. Fitch, E. Suard, and K. Prassides, Chem. Commun. **2008**, 5607 (2008).

[15] T. M. McQueen, Q. Huang, V. Ksenofontov, C. Felser, Q. Xu, H. Zandbergen, Y. S. Hor, J. Allred, A. J. Williams, D. Qu *et al.*, Phys. Rev. B **79**, 014522 (2009).

[16] S. Margadonna, Y. Takabayashi, Y. Ohishi, Y. Mizuguchi, Y. Takano, T. Kagayama, T. Nakagawa, M. Takata, and K. Prassides, Phys. Rev. B **80**, 064506 (2009).

[17] S. Tan, Y. Zhang, M. Xia, Z. Ye, F. Chen, X. Xie, R. Peng, D. Xu, Q. Fan, H. Xu *et al.*, Nat. Mater. **12**, 634 (2013).

[18] J.-F. Ge, Z.-L. Liu, C. Liu, C.-L. Gao, D. Qian, Q.-K. Xue, Y. Liu, and J.-F. Jia, Nat. Mater. **14**, 285 (2014).

[19] E.-W. Scheidt, V. R. Hathwar, D. Schmitz, A. Dunbar, W. Scherer, F. Mayr, V. Tsurkan, J. Deisenhofer, and A. Loidl, Eur. Phys. J. B **85**, 1 (2012).

[20] T. Hatakeda, T. Noji, T. Kawamata, M. Kato, and Y. Koike, J. Phys. Soc. Jpn. **82**, 123705 (2013).

[21] M. Burrard-Lucas, D. G. Free, S. J. Sedlmaier, J. D. Wright, S. J. Cassidy, Y. Hara, A. J. Corkett, T. Lancaster, P. J. Baker, S. J. Blundell *et al.*, Nat. Mater. **12**, 15 (2013).

[22] L. Zheng, M. Izumi, Y. Sakai, R. Eguchi, H. Goto, Y. Takabayashi, T. Kambe, T. Onji, S. Araki, T. C. Kobayashi *et al.*, Phys. Rev. B **88**, 094521 (2013).

[23] T. Noji, T. Hatakeda, S. Hosono, T. Kawamata, M. Kato, and Y. Koike, Phys. C (Amsterdam, Neth.) **504**, 8 (2014).

[24] S. Hosono, T. Noji, T. Hatakeda, T. Kawamata, M. Kato, and Y. Koike, J. Phys. Soc. Jpn. **83**, 113704 (2014).

[25] S. J. Sedlmaier, S. J. Cassidy, R. G. Morris, M. Drakopoulos, C. Reinhard, S. J. Moorhouse, D. O'Hare, P. Manuel, D. Khalyavin, and S. J. Clarke, J. Am. Chem. Soc. **136**, 630 (2014).

[26] H. Sun, D. N. Woodruff, S. J. Cassidy, G. M. Allcroft, S. J. Sedlmaier, A. L. Thompson, P. A. Bingham, S. D. Forder, S. Cartenet, N. Mary *et al.*, Inorg. Chem. **54**, 1958 (2015).

[27] D. Guterding, H. O. Jeschke, P. J. Hirschfeld, and R. Valentí, Phys. Rev. B **91**, 041112 (2015).

[28] U. Pachmayr, F. Nitsche, H. Luetkens, S. Kamusella, F. Brückner, R. Sarkar, H.-H. Klauss, and D. Johrendt, Angew. Chem. Int. Ed. **54**, 293 (2015).

[29] Y. P. Wu, D. Zhao, X. R. Lian, X. F. Lu, N. Z. Wang, X. G. Luo, X. H. Chen, and T. Wu, Phys. Rev. B **91**, 125107 (2015).

[30] P. Jeglič, J.-W. G. Bos, A. Zorko, M. Brunelli, K. Koch, H. Rosner, S. Margadonna, and D. Arčon, Phys. Rev. B **79**, 094515 (2009).

[31] M. Klanjšek, P. Jeglič, B. Lv, A. M. Guloy, C. W. Chu, and D. Arčon, Phys. Rev. B **84**, 054528 (2011).

[32] P. Jeglič, A. Potočnik, M. Klanjšek, M. Bobnar, M. Jagodič, K. Koch, H. Rosner, S. Margadonna, B. Lv, A. M. Guloy *et al.*, Phys. Rev. B **81**, 140511 (2010).

[33] C. P. Slichter, *Principles of Magnetic Resonance*, 3rd ed. (Springer, Berlin, 1996).

[34] A. Abragam, *Principles of Nuclear Magnetism* (Clarendon, Oxford, 2011).

[35] M. Goldman, Phys. Rev. **138**, A1675 (1965).

[36] K. W. Lee, C. H. Lee, and C. E. Lee, J. Phys. Soc. Jpn. **72**, 201 (2003).

[37] T. Imai, K. Ahilan, F. L. Ning, T. M. McQueen, and R. J. Cava, Phys. Rev. Lett. **102**, 177005 (2009).

[38] A. P. Dioguardi, J. Crocker, A. C. Shockley, C. H. Lin, K. R. Shirer, D. M. Nisson, M. M. Lawson, N. apRoberts Warren, P. C. Canfield, S. L. Bud'ko *et al.*, Phys. Rev. Lett. **111**, 207201 (2013).

[39] F. Hammerath, U. Gräfe, T. Kühne, H. Kühne, P. L. Kuhns, A. P. Reyes, G. Lang, S. Wurmehl, B. Büchner, P. Carretta *et al.*, Phys. Rev. B **88**, 104503 (2013).

[40] H.-J. Grafe, U. Gräfe, A. P. Dioguardi, N. J. Curro, S. Aswartham, S. Wurmehl, and B. Büchner, Phys. Rev. B **90**, 094519 (2014).

[41] I. I. Mazin, D. J. Singh, M. D. Johannes, and M. H. Du, Phys. Rev. Lett. **101**, 057003 (2008).

[42] H. Kontani and S. Onari, Phys. Rev. Lett. **104**, 157001 (2010).

[43] H.-Y. Choi, Phys. Rev. Lett. **81**, 441 (1998).

[44] A. Potočnik, A. Krajnc, P. Jeglič, Y. Takabayashi, A. Y. Ganin, K. Prassides, M. J. Rosseinsky, and D. Arčon, Sci. Rep. **4**, 4265 (2014).

[45] L. de' Medici, S. R. Hassan, M. Capone, and X. Dai, Phys. Rev. Lett. **102**, 126401 (2009).

[46] A. Tamai, A. Y. Ganin, E. Rozbicki, J. Bacsa, W. Meevasana, P. D. C. King, M. Caffio, R. Schaub, S. Margadonna, K. Prassides *et al.*, Phys. Rev. Lett. **104**, 097002 (2010).

[47] D. Arčon, P. Jeglič, A. Zorko, A. Potočnik, A. Y. Ganin, Y. Takabayashi, M. J. Rosseinsky, and K. Prassides, Phys. Rev. B **82**, 140508 (2010).

[48] H.-J. Grafe, D. Paar, G. Lang, N. J. Curro, G. Behr, J. Werner, J. Hamann-Borrero, C. Hess, N. Leps, R. Klingeler *et al.*, Phys. Rev. Lett. **101**, 047003 (2008).

[49] Y. Nakai, K. Ishida, Y. Kamihara, M. Hirano, and H. Hosono, J. Phys. Soc. Jpn. **77**, 073701 (2008).

[50] S. Kawasaki, K. Shimada, G. F. Chen, J. L. Luo, N. L. Wang, and G.-q. Zheng, Phys. Rev. B **78**, 220506 (2008).

[51] H. Mukuda, N. Terasaki, H. Kinouchi, M. Yashima, Y. Kitaoka, S. Suzuki, S. Miyasaka, S. Tajima, K. Miyazawa, P. Shirage *et al.*, J. Phys. Soc. Jpn. **77**, 093704 (2008).

[52] M. Yashima, H. Nishimura, H. Mukuda, Y. Kitaoka, K. Miyazawa, P. M. Shirage, K. Kihou, H. Kito, H. Eisaki, and A. Iyo, J. Phys. Soc. Jpn. **78**, 103702 (2009).

[53] H. Kotegawa, S. Masaki, Y. Awai, H. Tou, Y. Mizuguchi, and Y. Takano, J. Phys. Soc. Jpn. **77**, 113703 (2008).